

Superconducting $Y_1Ba_2Cu_3O_{7-y}$ thick films from nitrate pastes

L. STROM*, E. CARNALL, S. FERRANTI, J. MIR

Corporate Research Laboratories, Eastman Kodak Company, Rochester, NY 14650, USA

A novel technique for forming superconducting $Y_1Ba_2Cu_3O_{7-y}$ thick films by screen printing pastes made from spray-dried nitrate powders on alumina and magnesia is described. Manufacture and characterization of nitrate powders are discussed. A model based on dissolution of yttrium nitrate is proposed to explain the rheological and film-forming properties of the nitrate pastes. Low-viscosity pastes are found to give better performance in terms of printability and quality of prints. Barium carbonate formation can be avoided by use of the nitrate pastes and by firing in an oxygen atmosphere. Superconducting thick films were achieved on single-crystal (1 0 0) MgO ($T_0=77$ K) and on polycrystalline alumina with a prereacted barrier layer ($T_0=55$ K).

1. Introduction

High-transition-temperature superconducting ceramics have a very high potential for impacting technology in such a way that major advances in microelectronics, medicine and transportation may be possible. Since the discovery by Bednorz and Muller [1] in early 1986 of possible superconductivity at 35 K in $La_{5-x}Ba_xCu_5O_{15-y}$ ($x=1, 0.75; y>0$) and confirmation by Tanaka's and Chu's groups in December of 1986 [2], this potential has driven an unprecedented amount of work world-wide. The result has been phenomenal improvements in superconducting transition temperatures with the first improvement coming from substituting Sr for Ba which raised T_c to 40 K [2, 3]. Chu achieved a higher T_c of 90–100 K for a mixed phase system with overall composition of $Y_{1.2}Ba_{0.8}CuO_4$ [4]. The high superconductivity component of that system was found to be a new, distorted, oxygen-defect, perovskite phase with the composition of $Y_1Ba_2Cu_3O_{7-y}$ [5], hereafter referred to as YBC.

Superconducting thick films (films greater than 5 μm thick) may be of importance for microelectronic circuits [6]. They may allow for zero-resistance d.c. interconnects and low but finite a.c. impedance [7]. Delay times would be reduced slightly over copper traces at 77 K and the amount of heat generated would also be reduced [8]. This should result in faster and more closely packed circuits. Custom elements such as magnets should also be possible. Screen-printed thick films require less manufacturing steps and lower capital expense than methods normally used to produce monolithic or thin-film hybrid circuits [9, 10].

This report focuses on a method which is compatible with screen printing and has produced YBC films with a T_c of 97 ± 2 K and a complete transition

to zero resistivity (T_0) at 77 ± 2 K. The method deviates from the traditional screen-printing method in that a spray-dried powder of yttrium, barium and copper nitrates has been used in place of the calcined powder or metallo-organic. The powder was formed by dehydrating a fine spray of an aqueous nitrate solution of Y, Ba, and Cu in a spray drier. The powder was collected and mixed with water to form a blue pseudoplastic/thixotropic paste that could be coated on to a substrate by screen printing. Films were typically fired at 925–1075 °C, and subsequently annealed in oxygen at 400–600 °C. One advantage of this method is that no additives other than water have been necessary to convert the powder into a paste having good rheological and adhesive properties. It also circumvents the loss of oxygen that occurs when calcined YBC powder is in contact with some organic solvents [11] and decomposition when it is in contact with water [11, 12]. With this technique, solvent is evaporated before the YBC phase forms from the nitrates.

2. Experimental procedure

2.1. Aqueous nitrate solutions

Yttrium nitrate hexahydrate, barium nitrate and cupric nitrate (2.5 mol water) were dissolved in sufficient amounts of distilled water to effect complete dissolution and form aqueous nitrate solutions. Two types of solution were prepared: (1) solutions containing stoichiometric amounts of each cation in the mole ratio 1Y:2Ba:3Cu such that upon dehydration of the solution and firing, the YBC phase was obtained; (2) solutions containing 5 mol % excess Y and Cu. All solutions were filtered through a 0.45 μm membrane filter before spray drying.

* Present address: Hi-Tech Ceramics, Alfred, NY 14802, USA.

TABLE I

Spray-drying parameters	Sample ^a		
	1, Excess Y and Cu ^b	2, Stoichiometric	3, Ultrasonic ^c
Solution concentration (g ml ⁻¹)	0.15	0.12	0.15
Solution temperature (°C)	80	80	80
Preheat time (h)	1.5	2	1.5
Inlet air temperature (°C)	200	200	175
Outlet air temperature (°C)	100–105	90–95	95
Aspirator setting	3	3.1	3
Drying air flow (m ³ min ⁻¹)	0.3–0.35	0.3–0.35	0.3–0.35
Atomizing air pressure (MPa)	0.3	0.1	0.2
Pump rate setting	4	1.7	2.5
Pulsed air interval (s)	20	20	NA

^a This table is limited to samples discussed in the report. Several other powders have been made using similar spraying parameters.

^b Spraying Systems Atomizing Nozzle 2050 ss liquid and 64–5 ss air.

^c Sonnimist Ultrasonic Nozzle 600–2.

2.2. Powder formation

A Yamato Model GA-31 spray drier was used in its normal mode of operation to dehydrate the solutions. The particular parameters used in spray drying are shown in Table I. All the thick films were made using uncalcined powders. X-ray diffraction (XRD) of the powders was done using a Phillips diffractometer model PW1729 with CuK α radiation ($\lambda = 1.5405$ nm). A Jarrell–Ash Atomic Scan 2000 ICP (inductively coupled plasma) spectroscopy unit was used to analyse chemically the nitrate solutions, powders and films. Surface area of the powders was determined using multipoint BET analysis (nitrogen adsorption technique) and an equivalent spherical diameter estimate of the particle size was made. An Amray 1000 A scanning electron microscope (SEM) was used to show the actual size and shape of the spray-dried agglomerates and the component particles. When used in combination with the Kevex X-ray microanalysis unit, an estimate of the composition was also obtained. Thermogravimetric analysis (TGA) and differential scanning calorimetry (DSC) were run on the starting powders using a Du Pont Model 9900 thermal analysis unit. TGA of the individual nitrates was also run.

2.3. Paste formation and coating

Pastes were made from the dried powder by simply adding relatively small amounts of water (< 20 wt %) and mixing by hand. Isopropyl alcohol and formamide also were tried but appeared to give poorer pastes and therefore are not discussed further in this report. Paste viscosity, which can be controlled by the amount of water added, was measured with a Brookfield viscosimeter.

An AMI 432 semiautomatic screen printer was used in the off-contact mode to coat the YBC thick films on 96% alumina polycrystalline substrates. A patterned 200-mesh screen coated with a 15 μ m thick emulsion was used for testing the printability of the spray-dried nitrate pastes. Hand coating with a spatula was done when the substrate to be coated was smaller than that needed for screen printing. Although there is inherently more variability in this process, a great deal

was learned quickly and easily without using large amounts of materials.

Coatings were applied to polycrystalline 96% alumina and single crystal (100) magnesia. Polycrystalline alumina with barrier layers of zirconia and a prereacted barrier layer of YBC were also tried. Superconductor coatings were obtained on single-crystal magnesia, without a barrier layer. It was found that a barrier layer is necessary for superconducting films on 96% alumina due to diffusion of aluminium and/or silicon into the films.

2.4. Firing of films

Two different approaches were used to fire the thick films. One was a continuous heating profile from room temperature to the crystallization temperature of the superconductor phase (5 °C min⁻¹ to 200 °C, 10 °C min⁻¹ to 925 °C). The second was a two-step approach where the first step was low-temperature unidirectional heating at 550 °C and the second step was heating by convection at the crystallization temperature. The optimum crystallization temperature was 925 °C. These heat treatments were followed by an oxygen anneal between 400 and 600 °C. Heating profiles other than these are discussed in conjunction with the specific films on which they were used.

XRD has been used to study films at intermediate stages of the firing process to gain a better understanding of the reactions taking place. Film thicknesses were measured at intermediate steps by a Tencor Alpha scan 100 profilometer. Sheet resistance measurements were made on the fired thick films at room temperature with a Signatone four-point probe using a d.c. current of 4.53 μ A.

Resistance as a function of temperature was measured for several samples using the standard four-point probe technique. Contact was made to samples by melting pads of indium on the surface of the sample at low temperature (< 200 °C) and soldering a tinned copper wire to the indium pad. The measurements were typically made at 10 μ A and 750 Hz. A Janis cryostat was used to cool the samples down to < 5 K and resistance was plotted as a function of temperature during cooling and heating. The resistance

TABLE II

Material	Cation stoichiometry + 2S ^a			
	Y	Ba	Cu	Al
Stoichiometric solution	0.996 ± 0.023	2.03 ± 0.06	2.98 ± 0.06	—
Stoichiometric uncalcined powder	0.990 ± 0.022	2.04 ± 0.03	2.97 ± 0.08	—
Stoichiometric calcined powder	0.990 ± 0.025	1.99 ± 0.03	3.03 ± 0.12	—
Excess Y and Cu ^b uncalcined powder	1.01 ± 0.03	1.95 ± 0.05	3.05 ± 0.08	—
Excess Y and Cu ^b fired film	1.00 ± 0.03	1.95 ± 0.05	3.04 ± 0.09	0.0227 ± 0.0004

^a Scott Estes, Analytical Technology Division, Eastman Kodak.

^b If the Ba is normalized to 2 mol, the resulting composition is Y_{1.03}Ba₂Cu_{3.14}O_x.

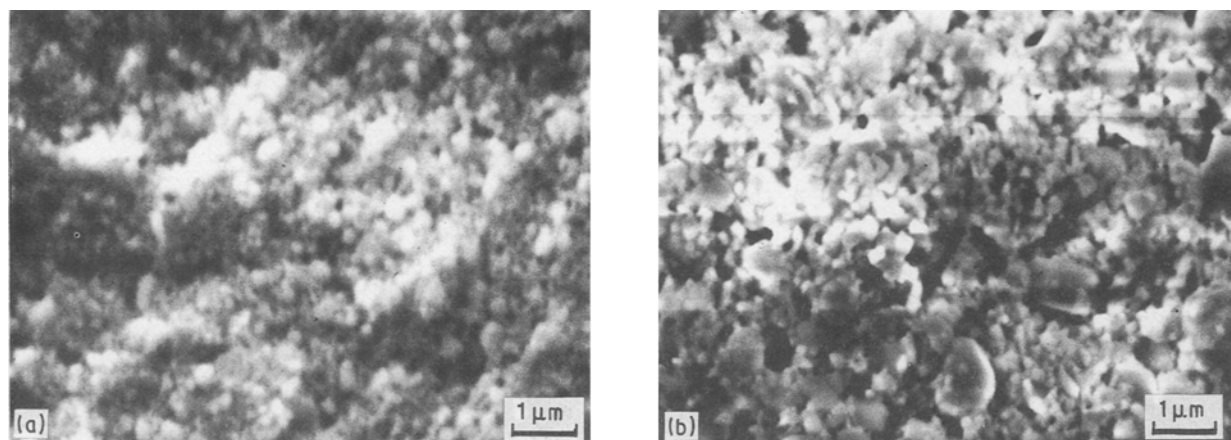


Figure 1 Scanning electron micrographs of dried films from (a) powder 1 and (b) powder 2 from Table I showing tendency of agglomerates to break down and form coatings of primary particles. Notice the particle size difference.

detectability limit is dependent on the current used but was typically $1 \times 10^{-5} \Omega$.

3. Results and discussion

3.1. Powder characteristics

It is widely recognized that characteristics of the starting powder can influence the final microstructure and properties of the ceramic piece, whether it be bulk or thick film. The most important characteristics are composition, crystallographic phase, surface area, decomposition behaviour, particle size and distribution. These characteristics are determined by the manner in which the aqueous nitrate solutions are spray-dried.

One major advantage of using the spray drier to obtain powders is a very close control of stoichiometry. Composition of YBC spray-dried nitrate powders was unchanged from the starting solution composition as shown by the data in Table II. This is an advantage over precipitation techniques, which often require trial and error to determine the amount of excess cations needed in solution in order to ensure stoichiometric powder [13, 14]. Excess cations are often needed to overcome differing rates of precipitation and/or varying solubility of precipitates. Theoretically, another advantage of spray drying is that chemical uniformity should extend down to the scale of the individual spray-dried particles that are formed from each droplet. This results from a more uniform and intimate mix of cations in solution than is possible

with mixtures of solids. The homogeneous mixture should be preserved by the rapid removal of solvent and simultaneous formation of particles.

Three types of particle were found in the spray-dried powders. The smallest or primary particles, shown in Fig. 1a and b, were generally $< 1 \mu\text{m}$. These particles were agglomerated into larger secondary particles shown in Fig. 2a. The secondary particles are believed to be derived from individual droplets of the sprayed nitrate solution. This is based upon their rounded nature and the correspondence of their size range with that calculated in the Appendix a ($3.6\text{--}10.7 \mu\text{m}$) for the type of nozzle, solution concentration, and pressure used. Secondary particles have a tendency to agglomerate into larger tertiary particles.

Composition of the secondary particles was found to vary within each particle. X-ray microanalysis spectra obtained from two different regions of the secondary particle in Fig. 2a are shown in Fig. 2b and c. Owing to the rough, curved surface of the particle, this analysis can only be used qualitatively. Although there is compositional variation within secondary particles, it is probably limited to that scale. The average composition of each particle should be the same because each one is derived from a separate drop of solution.

Surface area of the excess Y and Cu powder ($2.21 \text{ m}^2 \text{ g}^{-1}$) was found to be much higher than powder 2 ($0.66 \text{ m}^2 \text{ g}^{-1}$). The difference in surface area relates directly back to parameters used in spray drying. Two major factors that influence particle size

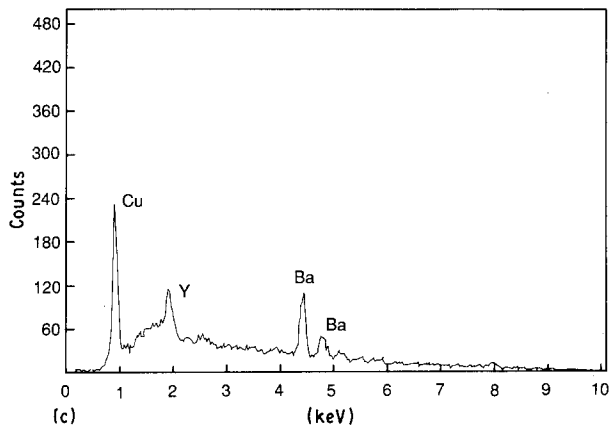
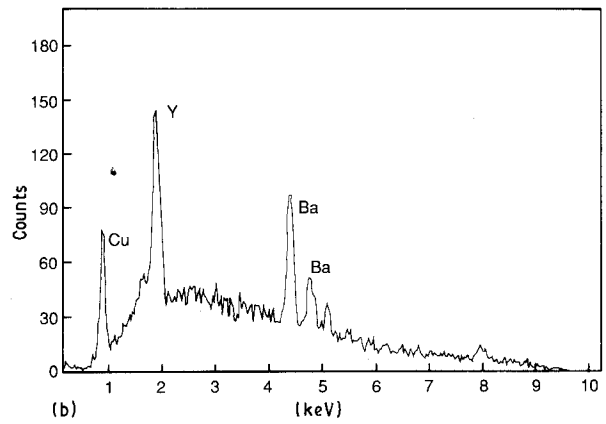
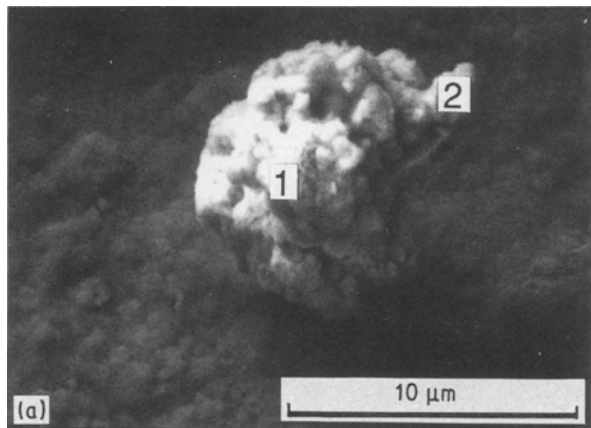


Figure 2 Scanning electron micrograph of a secondary particle from powder 1 (Table I) and X-ray spectra from regions (b) 1 and (c) 2 of the particle.

and, consequently, surface area are concentration of the solution used and size of the droplets that are dried. Droplet size is a function of nozzle, atomizing air pressure, and solution feed rate. From the parameters listed in Table I, it can be seen that the only difference between the two spray-drying runs that would result in larger particles for powder 2 is the atomizing air pressure used. The excess Y and Cu powder was made using higher atomizing air pressure. This resulted in smaller particles and therefore a higher surface area. From the surface area, an equivalent spherical diameter was estimated using an approximate density of 3.3 g cm^{-3} (based on the phases present in the powder). The diameter for the excess Y and Cu powder was estimated to be $0.41 \mu\text{m}$ and powder 2 was estimated to be $1.37 \mu\text{m}$. The size of the particles in the scanning electron micrograph (Fig. 1a) for the excess Y and Cu powder look to be close to the estimated value of $0.41 \mu\text{m}$. Powder 2 (Fig. 1b) is larger than the excess Y and Cu powder as predicted, but smaller than the estimated value.

Three crystallographic phases were found in the as-made spray-dried powders. Barium nitrate and copper trihydroxynitrate were the two major phases and yttrium monohydrate was a minor phase. Calcination of a stoichiometric powder for 24 h at 925°C resulted in orthorhombic YBC with little if any secondary phases present as shown in Fig. 3a. Spray-dried nitrate powders, therefore, may also be used for the traditional approach to thick films or tape casting. Superconducting properties of these powders were tested by making bulk samples from them. Resistance-temper-

ature data for a bulk sample are shown in Fig. 4b ($T_c = 95 \text{ K}$, $T_0 = 92 \text{ K}$).

TGA analysis of spray-dried nitrate powders revealed that the nitrates decompose individually rather than as a complex [15], as illustrated in Fig. 4. The initial weight loss was due to water loss below 150°C . It appears that the weight loss at $150\text{--}200^\circ\text{C}$ was from loss of the hydroxide group from the copper hydroxynitrate [16]. Decomposition of the remaining copper nitrate followed at approximately 280°C . The derivative peaks at 330 and 380°C were probably due to the decomposition of the yttrium nitrate hydrate [15]. Barium carbonate appeared to form from some barium nitrate at approximately 430°C and it decomposed at temperatures $> 800^\circ\text{C}$. The remaining unconverted barium nitrate decomposed in the range $550\text{--}700^\circ\text{C}$. TGA curves run in air were very similar to those run in O_2 . It is known from other studies, in which a mass spectrometer was used in conjunction with the TGA, that there is not a tight seal on the TGA and some air still flows through the system.

Analysis of the same powder described above with the DSC unit, which has a tighter seal, revealed a difference in behaviour between air and O_2 as shown in Fig. 5. The major difference between the two curves was that the endothermic peaks at 430 and 520°C were missing in the sample run in O_2 . The endothermic peak at 360°C was also more pronounced and the initial barium nitrate decomposition peak at 560°C was sharper for the sample run in O_2 . Peaks in the oxygen sample were shifted by about 10°C to higher temperatures. The difference in temperatures for the TGA runs versus the DSC was due to a kinetic effect caused by the difference in heating rates.

Spray-dried powders are made up of nitrates and hydrated nitrates with no organic ligands. C must be picked up from the atmosphere in order for barium carbonate to form. Firing under a pure O_2 atmosphere does not allow for any carbonate formation, and the peaks in the DSC curve for this reaction were missing (430 , 520°C). XRD of films fired to approximately 600°C in air compared with O_2 have a distinct

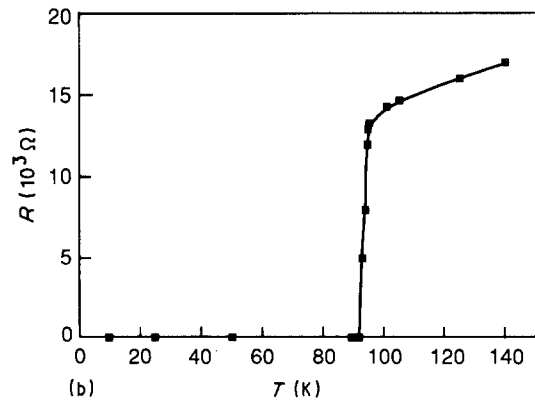
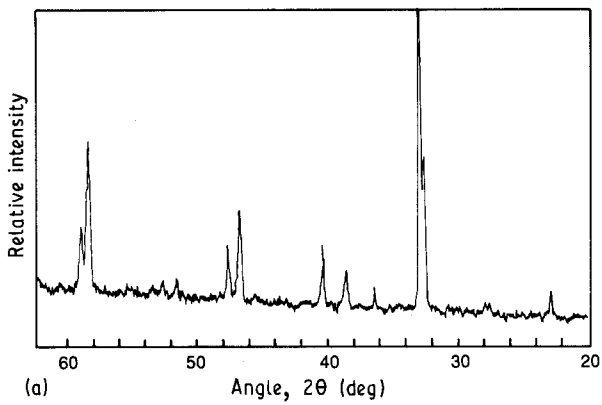


Figure 3 (a) XRD pattern of calcined YBC nitrate powder. (b) Resistance as a function of temperature for a bulk-sintered sample made from powder shown in (a).

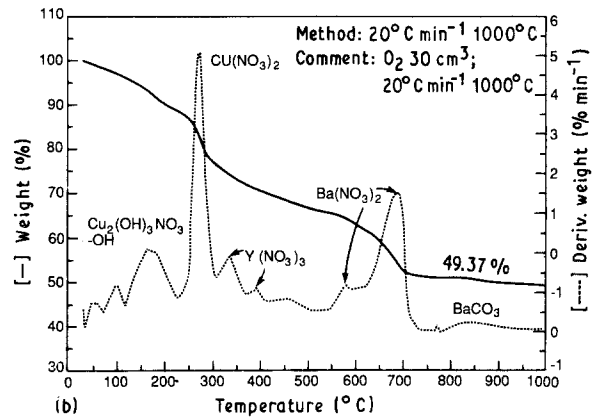
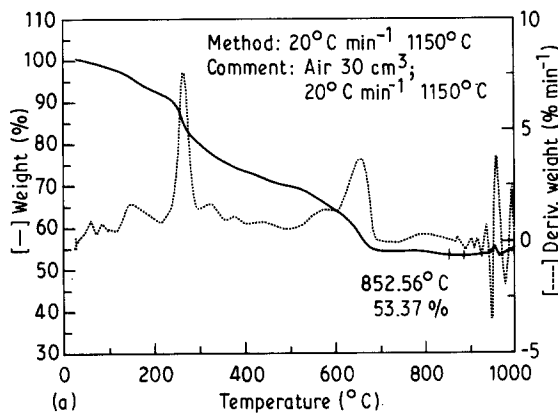


Figure 4 Thermogravimetric analysis of spray-dried nitrate powders indicating decomposition of the individual nitrates rather than a complex. (a) In air; (b) in O_2 .

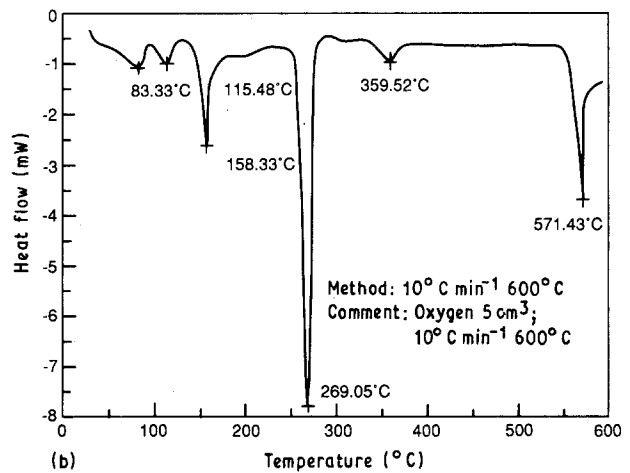
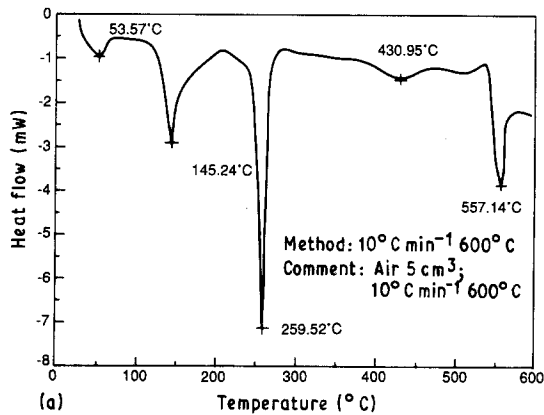


Figure 5 Differential scanning calorimetry of nitrate powders (a) in air and (b) in O_2 . Differences between curves believed to be due to a lack of $BaCO_3$ formation when fired in oxygen.

difference in the phases present, as shown in Fig. 6. The film fired in O_2 shows predominantly barium nitrate and a small amount of barium carbonate, which is probably the result of some air leakage. The film fired in air shows barium carbonate as the major phase with a small amount of an unknown phase also present.

Thick films fired in air require a temperature $> 800^\circ C$ to completely decompose the barium car-

bonate. Several researchers have theorized that avoiding barium carbonate would make possible lower reaction temperatures for forming YBC, and some have suggested using nitrates for that reason [17]. They have not discussed the need to fire in O_2 , however, to avoid the pick-up of carbon from air. We and other researchers [18] have found, however, that high temperatures are still necessary for adhesion of the film to the substrate.

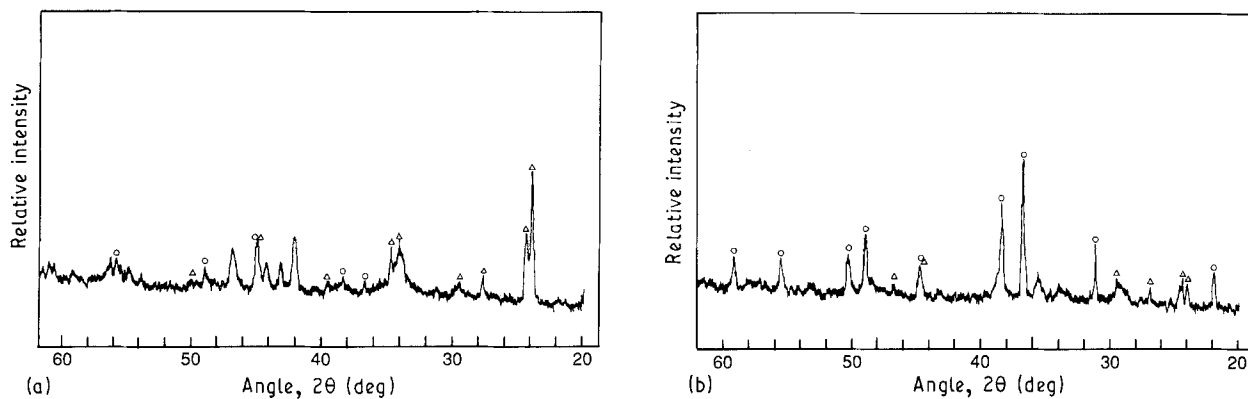


Figure 6 XRD patterns for films fired (a) in air and (b) in O_2 . Films fired in air appear to be absorbing CO_2 from the atmosphere and forming $BaCO_3$. Films fired in oxygen remain as $Ba(NO_3)_2$. (\circ) $Ba(NO_3)$, (\triangle) $BaCO_3$.

3.2. Film formation

When small amounts of water (< 20 wt %) were added to the spray-dried powders and mixed, a paste formed which appeared uniform in colour and texture. A comparison of the XRD patterns of dry powder and a newly made paste coated on a glass slide and X-rayed while wet showed that the yttrium nitrate dissolved. It is theorized that this breaks down the secondary particles and allows the less soluble barium nitrate and insoluble copper hydroxynitrate particles to move freely in a concentrated yttrium nitrate solution. When the paste was dried at room temperature and examined by XRD, the yttrium nitrate reprecipitated. From scanning electron micrographs of the dried pastes shown in Fig. 1a and b, it can be seen that the secondary particles broke down, creating a coating of the primary particles.

Dissolution and reprecipitation of the yttrium nitrate would have both positive and negative effects. Compositional variation due to migration of yttrium while in the liquid state is the major drawback. A positive aspect of this behaviour, however, is the ability of the yttrium to act as an adhesive agent in place of the glass frits often used in thick film compositions. In the case of the yttrium nitrate, it dissolves at room temperature and coats the copper hydroxynitrate and barium nitrate. Upon reprecipitation, the yttrium nitrate acts to hold these particles together and adhere them to the substrate. If the yttrium nitrate is indeed acting as a binder, two advantages would be: (1) the overall loading of the film is the same – it is not diluted by a component which does not participate in conductivity; and (2) most glass formers (i.e. alumina, silica, boron oxide, germanium oxide) that could be used as a frit have been found to inhibit superconductivity when reacted with YBC. The yttrium being a component of the crystalline phase needed for conductivity means that reaction of the yttrium with the Ba and Cu to promote adhesion is not deleterious.

The three pastes of widely different viscosity ($0.15\text{--}2.5 \times 10^6$ cP) were made from ground and sieved powder 2. Viscosity of nitrate pastes decreases both with increased amounts of water and with increased shear rate. One of the benefits of using nitrate pastes is the ease of controlling the viscosity by simply adjusting the water content. Another advantage of

using nitrate pastes is that additives are not required to improve the rheological properties for screen printing because the pastes are already pseudoplastic. All three pastes were easily screen-printed even though they are of widely different viscosities. The two lower viscosity pastes did exhibit better printing properties; the patterns printed from them had fewer defects. It appears that even lower viscosity nitrate pastes than those used in this study may be used for screen printing.

The screen-printed films were fired in air using both the two-step and continuous heat treatments. Lower viscosity pastes gave better performance in terms of printability, quality of prints and cracking, provided a sufficiently slow heating rate was used to allow for the controlled escape of water and other decomposition products. The comparison between continuous firing and a two-step heat treatment with the first step being unidirectional was not clear. It is believed, however, that unidirectional heating may enhance adhesion of the film to the substrate by promoting densification along the thickness of the film over lateral shrinkage.

The screen-printed films discussed above were coated on alumina because it is the standard substrate used for thick-film circuits. The majority of industrial thick-film pastes have been formulated for this substrate (i.e. the thermal expansion coefficients are compatible and the chemistry is formulated to have minimum interaction with the substrate). The alumina substrates interact with YBC thick films, however. A thick film made from the excess Y and Cu powder and coated on alumina was flaked off from the substrate leaving a green $Y_2Ba_1Cu_1O_x$ (211) [19] layer that often forms at the film/substrate interface. Chemical analysis of the removed film showed a large increase in the aluminium content over the starting powder (see Table II). A large amount of aluminium is diffusing into these films past even the interfacial reaction layer.

There are at least three possible routes for minimizing the interaction of the YBC films with the substrate. One approach is to lower the overall crystallization temperature. Another approach is to coat a barrier layer on the alumina to prevent the diffusion. These barrier layers are currently being developed, and a prereacted YBC barrier layer has been found to be successful for thick films. The third

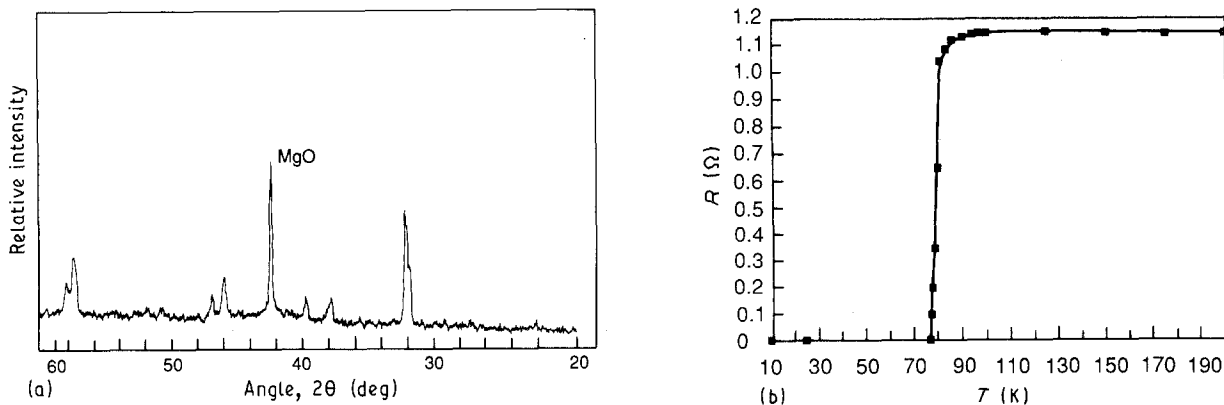


Figure 7 YBC thick film from powder 1 (Table I) on single-crystal MgO. (a) XRD pattern shows well-crystallized YBC with orthorhombic splitting. (b) Resistance as a function of temperature for sample in (a) $T_c = 97 \pm 2$ K, $T_0 = 77 \pm 2$ K.

approach that also has proved successful is using substrates other than alumina. Magnesia, zirconia and strontium titanate are viable candidates. Magnesia is especially attractive because its thermal expansion coefficient is close to that of YBC (13.5 compared with 12.0 p.p.m. $^{\circ}\text{C}^{-1}$) and it has a low dielectric constant compared to strontium titanate. The first two approaches are preferred because they would allow the use of alumina substrates and therefore be more compatible with thick-film resistors, dielectrics, etc., currently in use.

Superconducting thick films were made by hand-coating pastes on single-crystal (100) magnesia. The first superconducting thick film was made from the excess Y and Cu powder. The film was given a unidirectional heat treatment followed by a high-temperature treatment of 925°C for 15 min in air. After the high-temperature treatment, the film was cooled slowly to room temperature. The XRD pattern in Fig. 7a shows well-crystallized orthorhombic YBC and small amounts of secondary phases. The sheet resistance was $5 \Omega/\square$. The film was then oxygen-annealed for 1 h at approximately 600°C and cooled slowly to room temperature. The sheet resistance and XRD pattern of the annealed film were basically unchanged. Resistance as a function of temperature was measured and the graph is shown in Fig. 7b. The film has a T_c of 97 ± 2 K and achieved zero resistance (T_0) at 77 ± 2 K. It is believed that this curve can be drastically improved because the film contained both a green secondary phase (211) and several cracks. Other superconducting films have been made on single-crystal magnesia with stoichiometric YBC pastes but had transitions of slightly inferior quality.

Based upon the work of other researchers, it may be necessary to use an excess of Cu due to the formation of Cu-containing precipitates when YBC is coated on and reacted with magnesia, alumina, silica, zirconia and strontium titanate [20]. Segregation of dissolved yttrium nitrate to the film/substrate interface during coating may also require an excess of Y to maintain bulk stoichiometry. Evidence of this segregation is the tendency for the green, Y-rich, 211 phase to form at the interface.

Other researchers have obtained superconducting thick films on alumina and do not mention the use of

barrier layers [18]. We have found, however, that a barrier layer is necessary.

A YBC paste, made from ultrasonically spray-dried nitrate solution, was coated on to alumina substrate and fired. The thickness of the film was approximately $30 \mu\text{m}$ after a 935°C treatment and decreased to approximately $10 \mu\text{m}$ after an additional $1050\text{--}1080^{\circ}\text{C}$ treatment. XRD patterns of the film showed some preferred orientation in the (001) plane or $\langle 001 \rangle$ direction. Long, black, needle-like features were found in the film similar to those noticed in the thin-film work and by Budhani *et al.* at UCLA [18]. Budhani found these features to be composed only of Y and Cu. A second layer of YBC was coated over the prereacted barrier layer. The film was fired for 30 min at 750°C , followed by an additional 5 min at 900°C . The film was cooled slowly in air and then annealed under flowing O_2 for 1.5 h at approximately 430°C . The T_c and T_0 for the film were 93 and 55 K, respectively. These samples confirm that a prereacted YBC barrier layer is beneficial for obtaining superconducting thick films on alumina. Further improvements and a greater understanding of the effect of powder characteristics and processing conditions are still needed, however.

4. Conclusion

A method for forming superconducting YBC thick films by screen printing pastes made from spray-dried nitrate powders on alumina and magnesia has been developed. The best films were obtained using a paste containing excess Y and Cu coated on single-crystal (100) magnesia.

Some understanding of the effect of spray-drying parameters on the characteristics of the powders has been gained. It should be possible to use this knowledge to engineer powders with desired characteristics, such as small particle size and narrow distribution. A model has been proposed to explain the rheological and film-forming properties of pastes made from spray-dried nitrate powders. Low-viscosity pastes give better performance in terms of printability and quality of prints.

It was found that use of a nitrate paste allows one to avoid barium carbonate if fired in an O_2 atmosphere.

High firing temperatures ($> 900^{\circ}\text{C}$) help the orthorhombic phase to form when slow cooling rates and a secondary oxygen anneal are used. The high temperatures help adhere the films to the substrates but also increase the opportunity for substrate interaction.

Use of a prereacted YBC barrier layer has proven useful for reducing substrate interactions, and thick films with a T_0 of 55 K on alumina have been obtained.

Although much work needs to be done, the potential of this novel technique for producing screen-printed superconducting circuits of YBC has clearly been demonstrated.

Appendix a

Calculations used to derive an expected particle size for spray-dried powders follow. Based on empirical information provided by Spraying Systems Inc., a solution with viscosity similar to water sprayed with 40–100 p.s.i. (10^3 p.s.i. = 6.89 N mm^{-2}) through the 2050ss liquid nozzle should yield droplets of 20–60 μm diameter.

Droplet size

$$\begin{aligned} 4/3\pi r^3 &= 4/3\pi \left(\frac{60\ \mu\text{m}}{2} \right)^3 \\ &= 0.113 \times 10^6\ \mu\text{m}^3 \\ &= 0.113 \times 10^{-6}\ \text{ml} \end{aligned} \quad (\text{A1})$$

Approximate concentration of the excess Y and Cu solution was $0.15\ \text{g ml}^{-1}$.

$$\begin{aligned} 0.15\ \text{g ml}^{-1} \times 0.113 \times 10^{-6}\ \text{ml/droplet} \\ = 1.70 \times 10^{-8}\ \text{g/droplet} \end{aligned} \quad (\text{A2})$$

Approximate density of spray-dried powder based on phases shown to be present by XRD is $3.3\ \text{g cm}^{-3}$.

Particle size

$$1.70 \times 10^{-8}\ \text{g} / 3.3\ \text{g cm}^{-3} = 5.14 \times 10^{-9}\ \text{cm}^3 \quad (\text{A3})$$

Particle radius

$$1.07 \times 10^{-3}\ \text{cm} = 10.7\ \mu\text{m} \quad (\text{A4})$$

Similarly, a 20 μm diameter droplet would yield a particle with a radius equal to 3.57 μm .

References

1. J. G. BEDNORZ and K. A. MULLER, *Z. Phys. B* **64** (1986) 189.
2. D. R. CLARKE, *Adv. Ceram. Mater.* **2** (1987) 273–292.
3. R. J. CAVA *et al.*, *Phys. Rev. Lett.* **58** (1987) 408.
4. R. DAGANI, *Chem. Engng News* **65** (1987) 7.
5. F. BEECH *et al.*, *Phys. Rev. B* **35** (1987) 8778.
6. K. HARTLEY, *Sci. News* **132** (1987) 106.
7. P. CAMPBELL, *Nature* **330** (1987) 21.
8. "IEEE Satellite Telecast Conference on Superconductivity", 15–16 September 1987.
9. R. A. RIKOSKI, "Hybrid Microelectronic Circuits: The Thick Film" (Wiley Interscience, New York, 1973).
10. C. A. HARPER, "Handbook of Thick Film Hybrid Microelectronics" (McGraw-Hill, New York, 1974).
11. K. G. FRASE *et al.*, *Adv. Ceram. Mater.* **2** (1987) 698.
12. R. L. BARNS and R. A. LAUDISE, *Appl. Phys. Lett.* **51** (1987) 1373.
13. H. H. WANG *et al.*, *Inorg. Chem.* **26** (1987) 1474.
14. M. J. CIMA and W. E. RHINE, *Adv. Ceram. Mater.* **2** (1987) 329.
15. G. PAZ-PUJALT, private communication, April 1987.
16. J. MU and D. D. PERLMUTTER, *Thermochim. Acta* **56** (1982) 253.
17. S. DAVISON *et al.*, to be published.
18. R. C. BUDHANI *et al.*, *Appl. Phys. Lett.* **51** (1987) 1277.
19. Y. KITANO *et al.*, *Jpn. J. Appl. Phys. Lett.* **26** (1987) L394.
20. M. GURVITCH and A. T. FIORY, *Appl. Phys. Lett.* **51** (1987) 1027.

Received 18 September 1989
and accepted 9 April 1990